Journal of Alloys and Compounds 489 (2010) 421–423

Contents lists available at ScienceDirect

Journal of Alloys and Compounds

journal homepage: www.elsevier.com/locate/jallcom

Isothermal section of the Er–Fe–Al ternary system at 800 °C

M. Jemmali [a], S. Walha [b], M. Pasturel [c], O. Tougait [c], R. Ben Hassen [a,*], H. Noël [c]

[a] Unité de Recherche de Chimie des Matériaux, ISSBAT, Université de Tunis ElManar 9, Avenue Dr. Zoheir Safi, 1006 Tunis, Tunisia
[b] Laboratoire des Sciences des Matériaux et d'Environnement, Faculté des Sciences de Sfax, BP 1171, 3000 Sfax, Tunisia
[c] Laboratoire de Chimie de Solide et Matériaux, Sciences Chimiques de Rennes, UMR 6226 CNRS-Université Rennes 1, Avenue du Général Leclerc, 35042 Rennes, France

ARTICLE INFO

Article history:
Received 20 July 2009
Received in revised form
23 September 2009
Accepted 24 September 2009
Available online 4 October 2009

Keywords:
Intermetallics
Rare earth
Phase diagram
Erbium

ABSTRACT

Physico-chemical analysis techniques, including X-ray diffraction and Scanning Electron Microscope–Energy Dispersive X-ray Spectroscopy, were employed to construct the isothermal section of the Er–Fe–Al system at 800 °C. At this temperature, the phase diagram is characterized by the formation of five intermediate phases, $ErFe_{12-x}Al_x$ with $5 \leq x \leq 8$ ($ThMn_{12}$-type), $ErFe_{1+x}Al_{1-x}$ with $-0.2 \leq x \leq 0.75$ ($MgZn_2$-type), $ErFe_{3-x}Al_x$ with $0.5 < x \leq 1$ ($DyFe_2Al$-type), $Er_2Fe_{17-x}Al_x$ with $4.74 \leq x \leq 5.7$ ($TbCu_7$-type) and $Er_2Fe_{17-x}Al_x$ with $5.7 < x \leq 9.5$ (Th_2Zn_{17}-type), seven extensions of binaries into the ternary system; $ErFe_xAl_{3-x}$ with $x < 0.5$ (Au_3Cu-type), $ErFe_xAl_{2-x}$ with $x \leq 0.68$ ($MgCu_2$-type), $Er_2Fe_xAl_{1-x}$ with $x \leq 0.25$ (Co_2Si-type), $ErFe_{2-x}Al_x$ with $x \leq 0.5$ ($MgCu_2$-type), $ErFe_{3-x}Al_x$ with $x \leq 0.5$ (Be_3Nb-type), $Er_6Fe_{23-x}Al_x$ with $x \leq 8$ (Th_6Mn_{23}-type), and $Er_2Fe_{17-x}Al_x$ with $x \leq 4.75$ (Th_2Ni_{17}-type) and one intermetallic compound; the $ErFe_2Al_{10}$ ($YbFe_2Al_{10}$-type).

1. Introduction

This paper reports a continuation of the systematic investigations of the ternary systems on the basis of iron with contribution of rare earth elements (RE) and aluminium. So far, phase diagrams of La–Fe–Al system have been completely or partly constructed [1].

With the present study we have extended our interest to the case of a heavy rare earth metal in the Fe–Al matrix. Up to now the Er–Fe–Al ternary system was not studied in the whole concentration range, but some compounds were studied as isostructural members of larger series in order to investigate their physical properties [2–4].

The literature contains mainly reports about ternary compounds with stoichiometric compositions, which belong to solid solution based on binary compounds. The only known compound with well-defined stoichiometry is $ErFe_2Al_{10}$ [5]. Intermediate solid solutions are reported for $ErFe_xAl_{2-x}$ ($x \leq 0.68$), $ErFe_{2-x}Al_x$ ($x \leq 0.5$), both crystallizing in the cubic $MgCu_2$-type structure and $ErFe_{1+x}Al_{1-x}$ ($-0.2 \leq x \leq 0.25$) adopting the hexagonal $MgZn_2$-type structure [6], along the $ErAl_2$–$ErFe_2$ section. The compound $Er_6Fe_{20.3}Al_{2.7}$ was studied as part of the $Er_6Fe_{23-x}Al_x$ [7] extension into the ternary system. Three single phases in the homogeneity range of $ErFe_{12-x}Al_x$ ($ThMn_{12}$-type) with different stoichiometric compositions, $ErFe_7Al_5$, $ErFe_4Al_8$ and $ErFe_6Al_6$ have been described on the basis of their crystal structure refinement [2,8,9] and magnetic properties [3,4]. Two phases with different stoichiometric compositions $Er_2Fe_{11}Al_6$ and $Er_2Fe_{13.2}Al_{3.8}$ have been described by Zarechnyuk et al. [7] as independent compounds with different types of structure. They belong to the $Er_2Fe_{17-x}Al_x$ homogeneity range that has been extensively studied [10]. In this solid solution, as the Al content increases the 2/17H (hexagonal Th_2Ni_{17}-type structure) phase transforms, usually via the 1/7H (hexagonal $TbCu_7$ type structure) phase, into the 2/17R (rhombohedral Th_2Zn_{17}-type structure) phase [10].

The binary boundary erbium–iron, erbium–aluminium and iron–aluminium systems were accepted from a compilation of binary alloy phase diagrams by Massalski [11]. Table 1 summarizes the crystallographic data on unary and binary phases relevant to the present study [12–22].

As part of our systematic search of new interesting intermetallic compounds in this area, we present the results of the systematic investigation of the isothermal section at 800 °C; of the Er–Fe–Al phase diagram, in the whole concentration range.

2. Experimental details

The present investigation was carried out by preparing 90 samples, having masses of about 500 mg. The samples were synthesized using direct arc melting of the constituent metals (purity: Er = 99.8 wt%; Fe = 99.9 wt%; Al = 99.99 wt%) in a water-cooled copper hearth under high purity argon gas. Zirconium–titanium alloy was used as an O_2 getter during the melting process. The weight losses were less than 1 wt%. After melting, all alloys were homogenized by annealing in evacuated silica tubes. Heat-treatments were performed in a resistance furnace at 800 °C for one week, followed by quenching in water. However due to the presence of several extended solid solutions, prolonged annealing time was necessary, for some samples. The structural analysis was carried out using X-ray powder diffraction (Inel CPS

* Corresponding author. Tel.: +216 98692745; fax: +216 71573526.
E-mail address: rached.benhassen@fss.rnu.tn (R. Ben Hassen).

0925-8388/$ – see front matter
doi:10.1016/j.jallcom.2009.09.152

Table 1
Crystallographic data of compounds of binary, Er–Fe, Fe–Al and Er–Al.

Compound	Structure type	Space group	Lattice parameters (Å)			Reference
			a	*b*	*c*	
Er_2Fe_{17}	$Ni_{17}Th_{17}$	$P6_3/mmc$	8.45(2)		8.32(2)	[12]
Er_6Fe_{23}	Th_6Mn_{23}	$Fm\bar{3}m$	12.01(1)			[13]
$ErFe_3$	Be_3Nb	$R\bar{3}m$	5.089(3)		24.473(2)	[12]
$ErFe_2$	Cu_2Mg	$Fd\bar{3}m$	7.283(1)			[12]
ErAl	DyAl	$PBcm$	5.801(1)	11.272(3)	5.57(2)	[14]
$ErAl_2$	$MgCu_2$	$Fd\bar{3}m$	7.79(1)			[15]
$ErAl_3$	Au_3Cu	$Pm\bar{3}m$	4.215(2)			[16]
Er_2Al	Co_2Si	$Pnma$	6.516(2)	5.015(1)	9.279(3)	[17]
Er_2Al_3	Zr_3Al_2	$P4_2/mnm$	8.123(3)		7.484(1)	[14]
$FeAl_3$	$FeAl_3$	$C2/m$	15.489(1) $\beta = 107.72^\circ$	8.083(1)	12.476(2)	[18]
Fe_2Al_5	Fe_2Al_5	$Cmcm$	7.675(2)	6.403(2)	4.203(2)	[19]
Al	Cu	$Fm\bar{3}m$	4.049264(2)			[20]
Fe(α)	W	$Im\bar{3}m$	2.8665(2)			[21]
Fe(γ)	Cu	$Fm\bar{3}m$	3.6599(1)			[21]
Fe(δ)	W	$Im\bar{3}m$	2.9315(1)			[21]
Er	Mg	$P6_3/mmc$	3.559(2)		5.592(2)	[22]

120 diffractometer, using Co Kα radiation). Identification of the phases was made by the comparison between the observed powder patterns and those calculated using the program powder cell [23]. The microstructure of the samples was studied on polished surfaces using a Jeol JSM 6400 Scanning Electron Microscope (SEM) and the composition of the phases was analyzed by Energy Dispersive X-ray Spectroscopy (EDS) with an Oxford Link-Isis Si/Li analyzer.

3. Results and discussion

The isothermal section of the Er–Fe–Al ternary system at 800 °C, depicted in Fig. 1, was constructed by the analysis of the X-ray diffraction patterns, scanning electron micrographic images and EDS elementary compositions allowing the identification of the various phases present in each sample.

On the Er–Al boundary system, a solid solubility of iron of 4 at.% and 9 at.%, has been observed in $ErAl_3$ and Er_2Al binaries, respectively, leading to the chemical formulae $ErFe_{0.1}Al_{2.9}$ and $Er_{13}Fe_{1.5}Al_5$. The solubility of Al in Er is evaluated to be about 10 at.%. This result differs from that mentioned in the Er–Al binary system, assessed in ref [24], where the solubility of Al in Er does not exceed 1 at.% at 800 °C. On the Fe–Al axis, our results obtained at 800 °C are in agreement with the published binary phase diagram [25]. No solubility of Er was detected for these binary phases. We have confirmed the existence of the four binary compounds in the Er–Fe system reported in the literature [12,13]. All the phases in this binary system form more or less extended solid solution at constant rare earth composition due to the substitution of iron by aluminium.

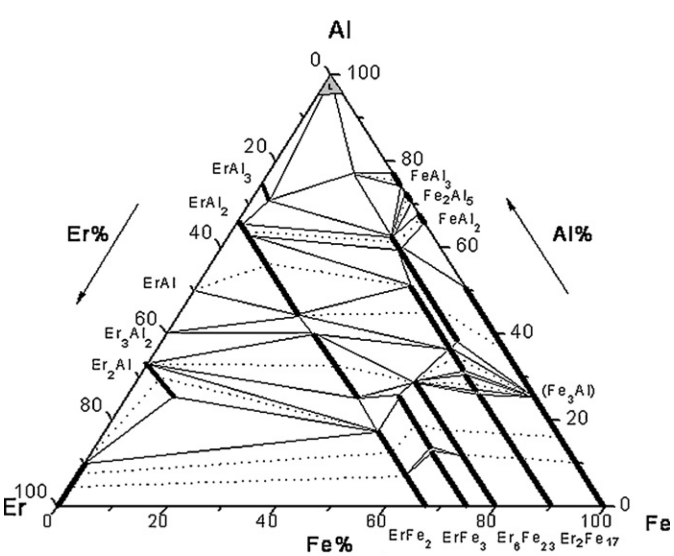

Fig. 1. Isothermal section of the Er–Fe–Al system at 800 °C: (1) $ErFe_2Al_{10}$, (2) $ErFe_{12-x}Al_x$, (3) $ErFe_{17-x}Al_x$, (4) $ErFe_{23-x}Al_x$, (5) $ErFe_{3-x}Al_x$, (6) $ErFe_{2-x}Al_x$, (7) $ErFe_{1+x}Al_{1-x}$ and (8) $ErFe_xAl_{2-x}$.

In this work, particular attention was given to the evaluation of the homogeneity ranges of the different phases, and of their equilibria. The type of structure reported for all the phases have been confirmed.

For the solid solution $Er_2Fe_{17-x}Al_x$, the transformations of the phases observed by Yanson et al. [10] are similar to the results found in the section at 800 °C. Indeed, microprobe analysis has revealed the formation of new phases with $Er_2Fe_8Al_9$ and $Er_2Fe_{11.8}Al_{5.2}$ estimated composition so that an extended solid solution, $Er_2Fe_{17-x}Al_x$, was identified along the 2:17 composition line, exhibiting three different crystal structures types depending on the substitution of Fe by Al in the binary compounds Er_2Fe_{17}. The analysis of the X-ray powder diffraction patterns revealed: in the range $0 \le x \le 4.75$, $Er_2Fe_{17-x}Al_x$ exhibits an hexagonal crystal structure (Th_2Ni_{17}-type), that transforms in the $TbCu_7$ hexagonal structure type for $x = 4.75$–5.7, in this range of concentration we have isolated the compound $Er_2Fe_{11.8}Al_{5.2}$. Its X-ray powder diffraction has been indexed in terms of an hexagonal unit cell $a = 4.956(1)$ Å and $c = 4.229(1)$ Å, indicating the $TbCu_7$-type structure. At high Al contents ($5.7 \le x \le 9.5$) the rhombohedral phase (Th_2Zn_{17}-type) is observed. A new intermediate phase was identified with $Er_2Fe_8Al_9$ composition, the X-ray powder diffraction present a strong similarity with the compound $Er_2Fe_{11}Al_6$ (Th_2Zn_{17}-type structure) reported by Zarechnyuk et al. [7]. Our result is consistent with the previous investigation carried out by Yanson et al. [10] at 500 °C, only the solubility range of the rhombohedral phase increases from 7.0 at.% to 9.5 at.% of Al at 800 °C.

The $ThMn_{12}$-type structure is stable within a significantly large homogeneity range for the solid solution $ErFe_{12-x}Al_x$. The limits of this solid solution confirm the previous limit compositions going from $ErFe_7Al_5$ to $ErFe_4Al_8$ [2,8]. Our results indicate the stability of the Th_6Mn_{23}-type structure at 800 °C within large range of composition, pointing to the chemical formula $Er_6Fe_{23-x}Al_x$ ($0 \le x \le 8$). The binary compounds $ErAl_2$ and $ErFe_2$ show, at constant erbium composition, a solubility of Al over three different regions: $ErFe_xAl_{2-x}$ ($x \le 0.68$), $ErFe_{2-x}Al_x$ ($x \le 0.5$) with the cubic $MgCu_2$-type structure and $ErFe_{1+x}Al_{1-x}$ ($-0.2 \le x \le 0.25$) that crystallizes in the hexagonal $MgZn_2$-type structure. The limits of the homogeneity domains are in agreement with those previously assessed at the same temperature [26].

Table 2
Crystallographic data of ternary Er–Fe–Al compounds and solid solutions stable at 800 °C.

Compound/composition (solid solution)	Structure type	Space group	Lattice parameters (Å)			Reference
			a	*b*	*c*	
$ErFe_2Al_{10}$	$YbFe_2Al_{10}$	*Cmcm*	8.948(2)	10.136(3)	8.988(1)	[5]
$Er_2Fe_{11}Al_6$ ($Er_2Fe_{17-x}Al_x$)	Th_2Zn_{17}	$R\bar{3}m$	8.79(2)		12.68(2)	[2]
$Er_2Fe_{13.2}Al_{3.8}$ ($Er_2Fe_{17-x}Al_x$)	Th_2Ni_{17}	$P6_3/mmc$	8.55(2)		8.4(2)	[2]
$Er_2Fe_{11.8}Al_{5.2}$ ($Er_2Fe_{17-x}Al_x$)	$TbCu_7$	$P6/mmm$	4.956(1)		4.229(1)	This work
$Er_2Fe_8Al_9$ ($Er_2Fe_{17-x}Al_x$)	Th_2Zn_{17}	$R\bar{3}m$	8.695(1)		12.692(3)	This work
$Er_6Fe_{20.3}Al_{2.7}$ ($Er_6Fe_{23-x}Al_x$)	Th_6Mn_{23}	$Fm\bar{3}m$	12.05(3)			[2]
$ErFe_4Al_8$ ($Er_1Fe_{12-x}Al_x$)			8.704(1)		5.037(1)	[8]
$Er_1Fe_7Al_5$ ($Er_1Fe_{12-x}Al_x$)	$ThMn_{12}$	$I4/mmm$	8.594(1)		4.981(1)	[9]
$ErFe_6Al_6$ ($Er_1Fe_{12-x}Al_x$)			8.619(5)		5.016(5)	[3]
$ErFe_{0.6}Al_{1.4}$ ($ErFe_xAl_{2-x}$)			7.65(2)			[26]
$ErFe_{0.3}Al_{1.7}$ ($ErFe_xAl_{2-x}$)	$MgCu_2$	$Fd\bar{3}m$	7.35(1)			[2]
$ErFe_{1.8}Al_{0.2}$ ($ErFe_{2-x}Al_x$)			7.753(1)			This work
$ErFe_{1.6}Al_{0.4}$ ($ErFe_{2-x}Al_x$)			7.308(2)			This work
$ErFe_{1.2}Al_{0.8}$ ($ErFe_{1+x}Al_{1-x}$)	$MgZn_2$	$P6_3/mmc$	5.4(1)		8.72(2)	[2]
ErFeAl ($ErFe_{1+x}Al_{1-x}$)			5.332(1)		8.683(2)	This work
$ErFe_2Al$ ($ErFe_{3-x}Al_x$)	$DyFe_2Al$	$P6_3/mmc$	5.156(2)		16.522(5)	This work
$Er_5Fe_{12.5}Al_{2.5}$ ($ErFe_{3-x}Al_x$)	Be_3Nb	$R\bar{3}m$	5.123(3)		24.691(7)	This work

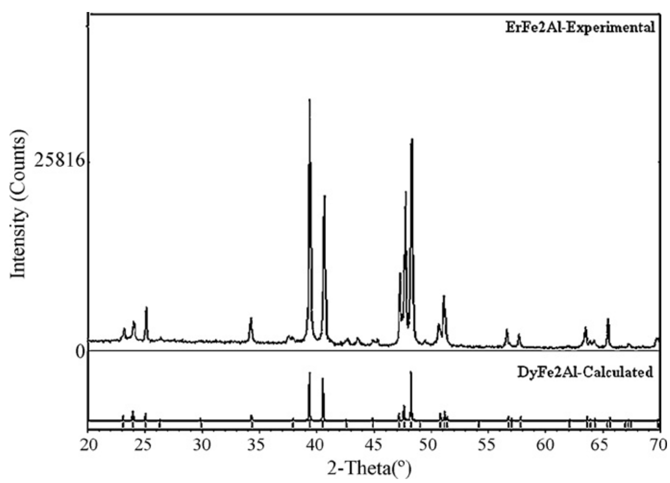

Fig. 2. Powder X-ray diffraction pattern for $ErFe_{3-x}Al_x$ ($2.5 < x \leq 1$) with a structure based in the $DyFe_2Al$-type (λ $K\alpha_{Co}$ = 1.798 Å).

The maximum of solid solubility of aluminium in $ErFe_3$ is about 25 at.%. A striking feature of this homogeneity range is the phase transformation sequence involving the apparition of another crystal structure at higher concentration of aluminium. For instance, the Be_3Nb-type structure (space group *R*-3*m*) covers the composition range from $ErFe_3$ to $Er_5Fe_{12.5}Al_{2.5}$ (25.6 at.% of Er, 62.5 at.% of Fe and 12.5 at.% of Al). As the aluminium content increases the powder pattern does not match with the rhombohedral phase, so that the new $ErFe_{3-x}Al_x$ ($0.5 \leq x < 1$) homogeneity range was indexed on the basis of a hexagonal unit cell. Comparison between simulated and experimental diagrams (Fig. 2) indicates that this solid solution is better described with the crystal structure of the $DyFe_2Al$ compound (space group $P6_3/mmc$).

The crystallographic data for the ternary Er–Fe–Al compounds and solid solutions formed at 800 °C are summarized in Table 2.

4. Conclusion

We have investigated and constructed the isothermal section of the Er–Fe–Al ternary system at 800 °C. This diagram is characterized by the formation of one ternary phase, five intermediate solid solutions and seven extensions into the ternary system of binary compounds. The substitution mechanisms are due to mutual substitution between Fe and Al.

References

[1] T. Weihua, L. Jingkui, R. Guanghui, G. Yongquan, Z. Yanming, J. Alloys Compd. 218 (1995) 127–130.
[2] W. Schafer, B. Barbier, I. Halevy, J. Alloys Compd. 303/304 (2000) 270–275.
[3] I.H. Hagmusa, E. Brock, F.R. de Boer, K.H.J. Buschow, J. Magn. Magn. Mater. 196–197 (1999) 625–626.
[4] O. Oleksyn, P. Schobinger-Papamantellos, J. Rodriguez-Carvajal, E. Bruck, K.H.J. Buschow, J. Alloys Compd. 257 (1997) 36–45.
[5] V.T. Thiede, T. Ebel, W. Jeitschko, J. Mater. Chem. 8 (1998) 125–130.
[6] H. Oesterreicher, J. Appl. Phys. 42 (1971) 5137–5143.
[7] O.S. Zarechnyuk, O.I. Vivchar, V.R. Ryabov, Visn. L'viv. Derzh. Univ. (Ser. Khim.) (1972) 14–16.
[8] K.H.J. Buschow, J.H.N. Vanvacht, W. Van Den Hoogenhof, J. Less-Common Met. 50 (1976) 145–150.
[9] I. Felner, J. Less-Common Met. 72 (1980) 241–249.
[10] T. Yanson, M. Manyako, O. Bodak, R. Cerny, K. Yvon, J. Alloys Compd. 320 (2001) 108–113.
[11] T.B. Massalski, Binary Alloy Phase Diagrams, vol. 2, second ed., ASM International, Materials Park, OH, 1990, pp. 1580–1581.
[12] K.H.J. Buschow, A.S. Van Der Goot, Phys. Status Solidi 35 (1969) 515–522.
[13] J.F. Herbst, J.J. Croat, B. van Laar, W.B. Yelon, J. Appl. Phys. 56 (1984) 1224–1226.
[14] G. Will, Z. Naturforsch. A 23 (1968) 413–416.
[15] E.E. Having, K.H.J. Buschow, H.J. Van Daal, Solid State Commun. 13 (1973) 621–627.
[16] K.H.J. Buschow, A.S. Van Der Goot, J. Less-Common Met. 24 (1971) 117–120.
[17] P.J. Black, Acta Crystallogr. 8 (1955) 43.
[18] K. Shubert, U. Rosler, M. Kluge, K. Anderko, L. Harle, Naturwissenschaften 40 (1953) 437.
[19] H.M. Otte, W.G. Montague, D.O. Welch, J. Appl. Phys. 34 (1963) 3149.
[20] R. Kohlhaas, P. Dunner, N. Schmitz-Pranche, Z. Angew. Phys. 23 (1967) 245.
[21] J.J. Hank, A.H. Daane, J. Less-Common Met. 3 (1961) 110–124.
[22] F.H. Spedding, A.H. Daane, K.H. Herrmann, Acta Crystallogr. 9 (1956) 559–563.
[23] G. Nolze, W. Kraus, Powder Cell for Windows, Version 2.2, Federal Institute for Materials Research and Testing, Berlin, 1999.
[24] K.A. Gschneidner Jr., F.W. Calderwood, in: T.B. Massalki (Ed.), Binary Alloy Phase Diagrams, vol. 1, second ed., ASM International, Materials Park, OH, 1990, pp. 144–146.
[25] U.R. Kattner, in: T.B. Massalki (Ed.), Binary Alloy Phase Diagrams, vol. 1, second ed., ASM International, Materials Park, OH, 1990, pp. 147–149.
[26] K.H.J. Buschow, N.V. Philips, J. Less-Common Met. 8 (1965) 209–212.